European Journal of Pharmacology 613 (2009) 10–18

Contents lists available at ScienceDirect

European Journal of Pharmacology

journal homepage: www.elsevier.com/locate/ejphar

Molecular and Cellular Pharmacology

Dipyridamole inhibits cobalt chloride-induced osteopontin expression in NRK52E cells

Tso-Hsiao Chen [a,b], Chia-Fang Chang [c,e], Shu-Chuan Yu [d], Jiueng-Chueng Wang [d], Cheng-Hsien Chen [a], Paul Chan [a], Horng-Mo Lee [c,d,e,*]

[a] Department of Internal Medicine, Taipei Medical University — Wan Fang Hospital, Taiwan
[b] Graduate Institute of Clinical Medicine, Taipei Medical University, Taipei, Taiwan
[c] Graduate Institute of Medical Sciences, Taipei Medical University, Taipei, Taiwan
[d] Department of Laboratory Medicine, Taipei Medical University — Wan Fang Hospital, Taiwan
[e] Department of Medical Laboratory Sciences and Biotechnology, Taipei Medical University, Taipei, Taiwan

ARTICLE INFO

Article history:
Received 2 September 2008
Received in revised form 12 March 2009
Accepted 23 March 2009
Available online 5 April 2009

Keywords:
Osteopontin
Dipyridamole
Heme oxygenase-1
NRK52E tubular cell

ABSTRACT

Osteopontin plays a pivotal role in the progression of interstitial fibrosis in renal ischemia. In the present study, rat renal tubular NRK52E cells treated with hypoxia mimetic cobalt chloride ($CoCl_2$) increased osteopontin production, and are associated with increased phosphorylation of Akt/PKB (protein kinase B) and p38 mitogen-activated protein kinase (p38MAPK). Furthermore, pretreatment of cells with *l*-N-acetylcysteine (an antioxidant) inhibited $CoCl_2$-stimulated osteopontin protein expression and p38MAPK phosphorylation, but not Akt/PKB phosphorylation. Pretreatment of cells with anti-inflammatory agents celecoxib, tanshinone IIA, and dipyridamole inhibited $CoCl_2$-induced osteopontin production paralleled by heme oxygenase-1 (HO-1) induction. Pretreatment of cells with tin protoporphyrin (a HO-1 inhibitor) or hemoglobin (a carbon monoxide scavenging agent) reversed dipyridamole inhibition of osteopontin expression. Moreover, transfection of HO-1 small interfering RNA (siRNA) reduced dipyridamole-stimulated mitogen-activated protein kinase phosphatase-1 (MKP-1) phosphorylation. Conversely, MKP-1 knockdown reversed dipyridamole inhibition of osteopontin expression. Taken together, these data suggest that dipyridamole may inhibit $CoCl_2$-induced osteopontin expression through HO-1 induction. Increased HO-1 may catalyze the conversion of heme into carbon monoxide, in turn carbon monoxide activates MKP-1. MKP-1 activation inhibits the p38MAPK signaling pathway that mediates $CoCl_2$-induced osteopontin production.

1. Introduction

Renal ischemia may induce tubular interstitial fibrosis. Hypoxia upregulates matrix production and decreases turnover in renal fibroblasts which are key events leading to tubulointerstitial fibrosis (Norman et al., 2000). Although the underlying mechanisms are not completely known, several observations suggest that osteopontin might be involved in the cellular response to ischemic injury (Basile et al., 2005; Choi et al., 2007). Osteopontin protein and gene expressions were elevated after ischemia and subsequent reperfusion in an *ex vivo* hemoperfusion model (Kossmehl et al., 2005). Osteopontin was upregulated after renal ischemia/reperfusion and was linked to interstitial fibrosis and renal failure (Lien et al., 2003). Knockout of osteopontin reduced post-ischemic macrophage infiltration and interstitial fibrosis in mice (Persy et al., 2003).

Osteopontin is a secreted glycoprotein, which was originally identified as a bone phosphoprotein secreted by the osteoid matrix (Ashkar et al., 2000). Osteopontin is also secreted by extra-osteous cell types, including renal tubular epithelial cells (Giachelli et al., 1994). Osteopontin is expressed at low levels in normal kidneys and is upregulated in kidney diseases, including renal ischemia/reperfusion (Lien et al., 2003), essential hypertension (Thomas et al., 1998), crescentic glomerulonephritis (Khanna et al., 2002; Lan et al., 1998), cisplatin-induced tubular injury (Iguchi et al., 2004); immunoglobulin A nephropathy, diffuse lupus nephritis, and diabetic nephropathies (Xie et al., 2001). Osteopontin also plays an important role in mediating fibrosis and has been considered a therapeutic target of renal fibrosis (Yoo et al., 2006).

Heme oxygenase (HO) catalyzes the rate-limiting step in heme degradation, resulting in the formation of iron, carbon monoxide, and biliverdin. Biliverdin is subsequently converted to bilirubin by biliverdin reductase. Three isoforms of the heme oxygenase (HO) enzyme have been described: an inducible isoform, HO-1, and two constitutively expressed isoforms, HO-2 and HO-3. Induction of HO-1 occurs as an adaptive and beneficial response to several injurious stimuli, and has been implicated in many clinically relevant disease

* Corresponding author. Graduate Institute of Medical Sciences, Taipei Medical University, 250 Wu-Hsing Street, Taipei 110, Taiwan. Tel.: +886 2 2736 1661x3316; fax: +886 2 2732 4510.
E-mail address: leehorng@tmu.edu.tw (H.-M. Lee).

0014-2999/$ – see front matter © 2009 Elsevier B.V. All rights reserved.
doi:10.1016/j.ejphar.2009.03.063

states including acute renal injury. HO-1 functions as a cytoprotective mechanism against inflammatory responses and reactive oxygen species insults through the anti-inflammatory action of its metabolite, carbon monoxide (CO), and the antioxidant activities of another metabolite, bilirulin (Otterbein and Choi, 2000).

Dipyridamole is a drug frequently used in nephrology clinics because it improves hemodynamic and thus proteinuria in a variety of kidney diseases (Levin, 1999; Nolin and Courteau, 1999). Dipyridamole is a nucleoside transport inhibitor (Hammond et al., 2004) and a non-selective phosphodiesterase inhibitor, which inhibits the degradation of cyclic AMP (cAMP) and cyclic GMP (cGMP) thereby increasing cellular levels of cAMP, and cGMP (Bender and Beavo, 2006). Dipyridamole also inhibits platelet function by blocking adenosine reuptake and degradation and thus exerts an antithrombogenic effect (Stafford et al., 2003). Dipyridamole inhibits proliferation and collagen synthesis in human aortic smooth muscle cells (Dubey et al., 1999), and inhibits the fibrogenic effect of peritoneal mesothelial cells and the accompanying accumulation of extracellular matrix in peritoneal fibrosing syndrome (Hung et al., 2001a,b,c). These inhibitory effects may contribute to retardation of renal interstitial fibrosis.

In the present study, we used the chemical ischemic agent, cobalt chloride ($CoCl_2$), to induce osteopontin production in NRK52E renal tubular epithelial cells. NRK52E renal epithelial cells were used as a cell model because osteopontin mRNA and protein expression in renal epithelial cells can be potently induced by injured kidney early in tubular interstitial fibrosis (Malyankar et al., 1997). We provide evidence that reactive oxygen species generation is involved in the induction of HO-1 and the suppression of $CoCl_2$-induced osteopontin expression. We demonstrate that dipyridamole suppresses osteopontin protein expression through HO-1 induction. HO-1 in turn catalyzes the degradation of heme into CO, which then suppresses $CoCl_2$-induced osteopontin expression via a mitogen-activated protein kinase phosphatase-1 (MKP-1) dependent mechanism.

2. Materials and methods

2.1. Materials

Affinity-purified polyclonal antibodies specific to rat HO-1, osteopontin, p38 mitogen-activated protein kinase (p38MAPK), Akt, and α-tubulin, and horseradish peroxidase-conjugated anti-mouse and anti-rabbit antibodies, and protein A beads, were obtained from Transduction Laboratory (Lexington, KY). All materials for sodium dodecyl sulfate polyacrylamide gel electrophoresis (SDS-PAGE) were obtained from Bio-Rad (Hercules, CA). 2′-Amino-3′-methoxyflavone (PD98059), pyrrolidine dithiocarbamate (PDTC), anthra(1,9-*cd*)pyrazol-6(2*H*)-one (SP600125), 2-(4-Morpholino)-8-phenyl-4*H*-1-benzopyran-4-one (Ly294002) and 4-(4-fluorophenyl)-2-(4-methylsulfinylphenyl)-5-(4-pyridyl)1*H*-imidazole (SB 203580) were purchased from Calbiochem (San Diego, CA). Dulbecco's modified Eagle medium (DMEM), fetal bovine serum, L-glutamine, sodium pyruvate, penicillin, and streptomycin were purchased from Life Technologies (Gaithersburg, MD). The 5-bromo-4-chloro-3-indolyl-phosphate/4-nitro blue tetrazolium (BCIP/NBT) substrate was purchased from Kirkegaard and Perry Laboratories (Gaithersburg, MD). Protease inhibitor cocktail tablets were purchased from Boehringer Mannheim (Mannheim, Germany). HO-1 and MKP-1 siRNA were purchased from Ambion (Austin, Texas).

2.2. Culture of NRK52E cells and preparation of cell lysates

NRK52E renal tubular epithelial cells were cultured in DMEM supplemented with 13.1 mM $NaHCO_3$, 13 mM glucose, 2 mM glutamine, 10% heat-inactivated fetal bovine serum, and penicillin (100 U/ml)/streptomycin (100 mg/ml). Cells were attached to a Petri dish after 24 h of incubation. Cells were plated at a concentration of 1×10^5 cells/ml and used for experiments when they reached 80% confluency. Cultures were maintained in a humidified incubator with 5% CO_2 at 37 °C. After reaching confluence, cells were treated with various concentrations of $CoCl_2$ in the presence or absence of dipyridamole or other inhibitors for the indicated time intervals and incubated in a humidified incubator at 37 °C. After incubation, cells were lysed by adding lysis buffer containing 10 mM Tris HCl (pH 7.5), 1 mM EGTA, 1 mM $MgCl_2$, 1 mM sodium orthovanadate, 1 mM dithiothreitol (DTT), 0.1% mercaptoethanol, 0.5% Triton X-100, and the protease inhibitor cocktails (at final concentrations of 0.2 mM PMSF, 0.1% aprotinin, and 50 μg/ml leupeptin). Cells adhering to the plates were scraped off using a rubber policeman and stored at −70 °C for further measurements.

2.3. Sodium dodecyl sulfate polyacrylamide gel electrophoresis (SDS-PAGE) and Western blotting

Electrophoresis were ordinarily carried out on different percentages of SDS-PAGE. Following electrophoresis, separated proteins on the gel were electro-transferred onto a polyvinydifluoride (PVDF) membrane. Nonspecific bindings were blocked with blocking buffer containing 5% fat-free milk powder in Tris-Buffered Saline with 1% Tween-20 (TBST) for 1 h at room temperature, followed by incubation with the primary antibody in blocking buffer for 2 h. The PVDF membrane was then incubated with an alkaline phosphatase-conjugated secondary antibody for 1 h. Subsequently, Western blots were developed with bromo-chloro-indoryl phosphate/nitro blue tetrazolium (BCIP/NBT) as the substrate.

2.4. Quantitative analysis of osteopontin production in the medium by enzyme-linked immunosorbent assay (ELISA)

Osteopontin in the culture supernatants was determined using the ELISA kit for rat osteopontin (Assay designs, Inc. Ann Arbor, MI) according to the manufacturer's instruction. Osteopontin concentrations in cell culture media are expressed in pg/ml.

2.5. Reverse-transcription polymerase chain reaction (RT-PCR) analysis of HO-1 messenger RNA (mRNA) levels

Total cellular RNA was extracted using phenol-guanidium isothiocyanate. Two micrograms of RNA was reverse-transcribed to complementary DNA (cDNA) by incubation with 2.5 mM of each dNTP, 2.5 μM random hexamer primers, 1 mM DTT, 20 U of an RNAsin ribonuclease inhibitor, and 100 U of Moloney murine leukemia virus reverse transcriptase. PCR amplification of HO-1 cDNA was performed as described by Alvarez-Maqueda et al. (2004). Briefly, 0.5 μM of each HO-1 specific primers (forward, 5′-TTCTTCACCTTCCCCAAC-3′, and reverse 5′-GCATAAAGCCCTACAGCAAC-3′), 400 μM of the four dNTPs, 5% methylsulfoxide, and 1 U of *Taq* DNA polymerase (Roche Diagnostics, Indianapolis, IN) were used. After an initial denaturation at 94.5 °C for 5 min, the PCR was performed for 45 cycles, each at 94.5 °C for 1 min, 60 °C for 2 min, and 72 °C for 3 min. The glyceraldehyde-3-phosphate dehydrogenase (G3PDH) gene was used as an internal control, and was amplified using the following primers: forward, 5′-CCACCCATGGCAAATTCCATGGC-3′, and reverse 5′-TCTAGACGGCAGGTCAGGTCCACC-3′. PCR products were separated on 1.2% agarose gels stained with ethidium bromide.

2.6. Measurement of intracellular reactive oxygen species generation

Intracellular reactive oxygen species generation was assessed using 2′,7′-dichlorodihydrofluescein diacetate (DCFH-DA) (Molecular Probes, Leiden, The Netherlands) as described by Chandel et al. (2000). Briefly, 5×10^6 NRK52E cells were cultured in Petri dishes and incubated with 10 μM DCFH-DA at 37 °C for 30 min. Cells were washed

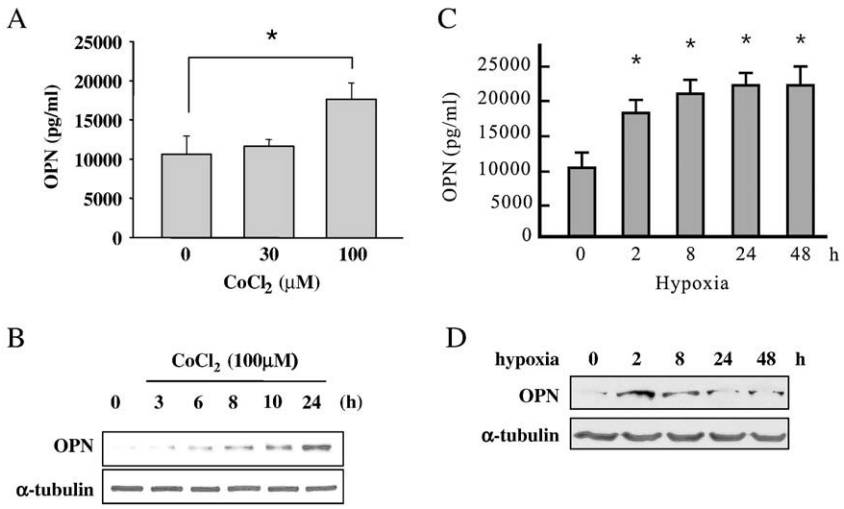

Fig. 1. Effects of $CoCl_2$ on osteopontin production and cell viability in cultured rat NRK52E renal tubular epithelial cells. A, After serum-starvation for 24 h, NRK52E cells were incubated in serum-free medium containing different concentrations of $CoCl_2$ for 24 h. Serum-free culture media were collected for quantitative assessment of osteopontin (OPN) secretion. B, Cells were lysed and cell lysates were immunoblotted with osteopontin (OPN) and α-tubulin specific antibodies. α-Tubulin expression served as equal loading control. C, A hypoxia model used Anaeropack (from Mitsubishi Gas Chemical Co., Tokyo, Japan) to generate 1% O_2 and 5% CO_2 incubation condition. NRK52E renal tubular epithelial cells were incubated under hypoxic condition, and hypoxic stimulus-induced osteopontin secretion in NRK-52E cells was quantitated. D, Hypoxic stimulus-induced osteopontin (OPN) protein expression was analyzed using Western blotting assay. Data in panels B and D are representative data that have been repeated twice with similar results. Data shown in panels A and C are the means ± S.D. for 3 independent experiments done in triplicate. *Statistical differences ($P<0.05$) compared to control.

and incubated with $CoCl_2$ (100 μM) in the presence or absence of dipyridamole (3 μM) for various periods of time. Reactive oxygen species in the cells oxidized DCFH-DA to a fluorescent product (DCF). The intracellular fluorescence of DCF was measured using flow cytometry. Data were normalized to fluorescence intensities obtained from the untreated control.

2.7. Statistical analysis

All data are expressed as the mean ± S.D. Statistical analysis was performed using one-way ANOVA among the groups, and Student's *t*-test was used to compare the separate groups. A difference between groups of $P<0.05$ was considered statistically significant.

3. Results

3.1. $CoCl_2$ induced osteopontin expression in NRK52E renal tubular epithelial cells

We first tested whether the chemical ischemic agent, $CoCl_2$, induced osteopontin production in NRK52E renal tubular epithelial cells by measuring osteopontin accumulation in culture media (Fig. 1A) and cellular osteopontin protein expression by Western blot analysis (Fig. 1B). Treatment of cells with $CoCl_2$ (30–100 μM) induced osteopontin expression in a dose-dependent manner, and the maximum response was observed at 100 μM (Fig. 1A). Concentration of $CoCl_2$ greater than 100 μM decreased the viable cell number as analyzed by 3-(4,5-dimethyl thiazol-2-yl)-2,5-diphenyl tetrazolium bromide (MTT) assay (data not shown). $CoCl_2$ at a concentration of 100 μM was used in subsequent experiments. Incubation of cells with $CoCl_2$ (100 μM) increased cellular osteopontin protein expression. Osteopontin protein level become detectable at 6 h after $CoCl_2$ was added and reached maximum at 24 h (Fig. 1B). In order to confirm that osteopontin is induced by hypoxia, cells were incubated under hypoxia condition (1% O_2 and 5% CO_2) and osteopontin secretion in culture media (Fig. 1C), and cellular osteopontin protein levels (Fig. 1D) at various time points were examined. Incubation of cells under hypoxic condition increased osteopontin production.

3.2. Roles of reactive oxygen species in $CoCl_2$-induced osteopontin expression in NRK52E cells

We next investigated whether $CoCl_2$-induced osteopontin protein expression was altered by treating of cells with *l*-N-acetylcysteine, which increases the endogenous antioxidant activity. As shown in Fig. 2A and B, when cells were pretreated with *l*-N-acetylcysteine prior to the addition of $CoCl_2$ (100 μM), pretreatment with *l*-N-acetylcysteine suppressed $CoCl_2$-induced osteopontin production in NRK52E cells. Similar effect was seen when another antioxidant, pyrrolidine dithiocarbamate (PDTC), was used to treat the cells (Fig. 2C). *l*-N-acetylcysteine (10 mM) and PDTC (30 μM) did not alter cell viability (data not shown). Next, we investigated whether $CoCl_2$ was able to alter intracellular reactive oxygen species levels in NRK52E cells using the reactive oxygen species-sensitive fluorescent probe, DCFH-DA. As shown in Fig. 2D $CoCl_2$ significantly increased intracellular reactive oxygen species levels in NRK52E cells. These data suggest that intracellular reactive oxygen species are involved in the induction of osteopontin by $CoCl_2$ in NRK52E cells. We next analyzed the signaling mechanisms by which $CoCl_2$ induces osteopontin expression using specific pharmacological inhibitors. As shown in Fig. 2E, inhibition of JNK by SP600125 did not inhibit $CoCl_2$-induced osteopontin protein expression. However, when cells were pretreated with SB203580 (10 μM) (an inhibitor of p38MAPK) or Ly294002 (20 μM), inhibitors of phosphatidylinositol 3-kinase (PI3-kinase), and then challenged with $CoCl_2$ for 24 h, SB203580 or Ly294002 significantly blocked $CoCl_2$-induced osteopontin expression (Fig. 2E). To confirm that $CoCl_2$ did activate the PI3-kinase and p38MAPK pathway, we examined whether $CoCl_2$ increased Akt/PKB (protein kinase B) and p38MAPK phosphorylation in NRK52E cells. Treatment of cells with $CoCl_2$ (100 μM) increased the levels of Akt/PKB and p38MAPK phosphorylation (Fig. 2F). Pretreatment of cells with *l*-N-acetylcysteine inhibited $CoCl_2$-stimulated p38MAPK phosphorylation, but not Akt/PKB phosphorylation (Fig. 2G).

3.3. Effects of anti-inflammatory agents on $CoCl_2$-induced OPN expression in NRK52E cells

To determine whether anti-inflammatory agents can suppress $CoCl_2$-induced osteopontin expression, NRK52E cells were pretreated

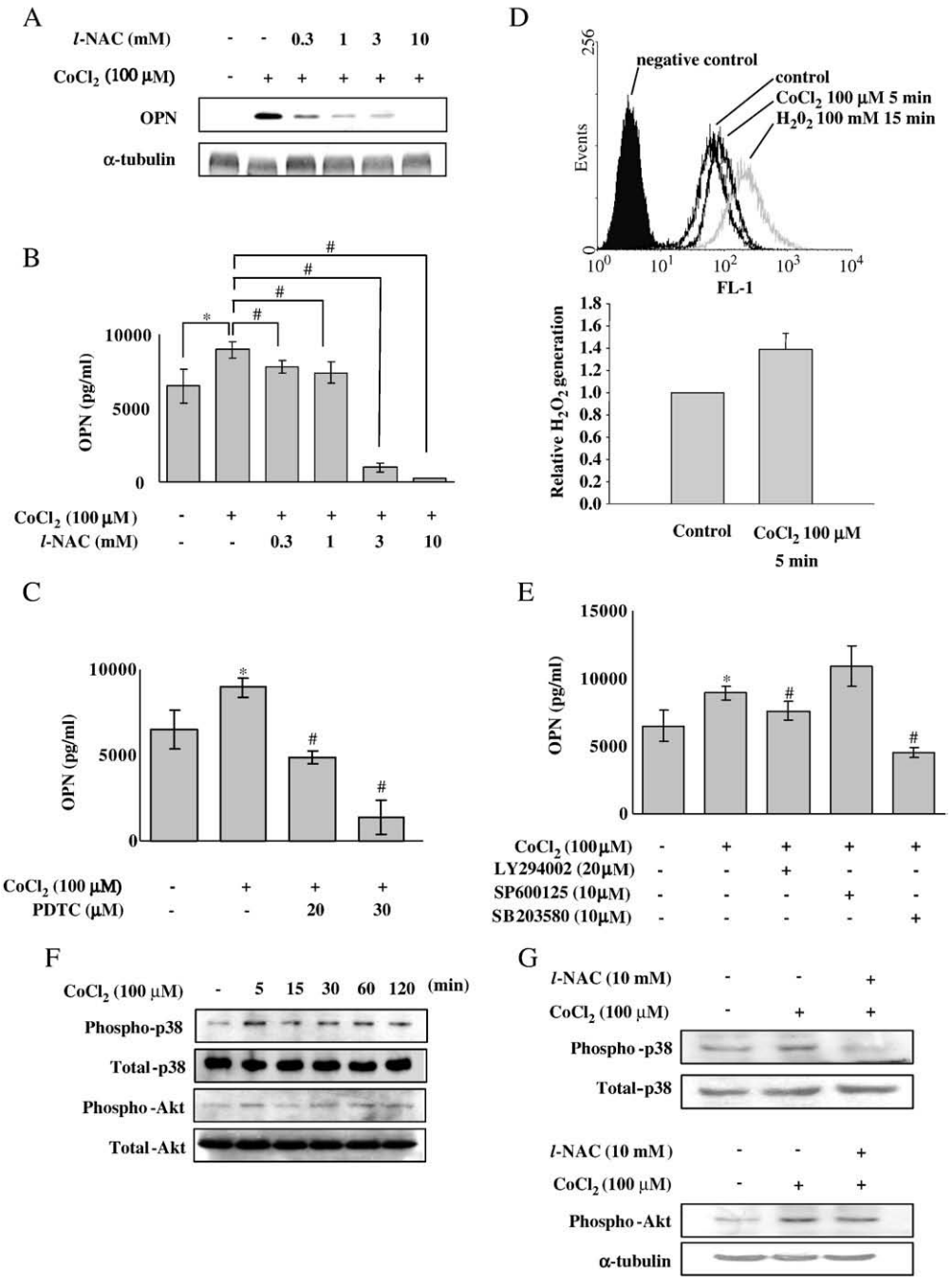

Fig. 2. Role of reactive oxygen species in $CoCl_2$-induced osteopontin production in NRK52E cells. Cells were pretreated with *l*-N-acetylcysteine (0.3–10 mM, *l*-NAC) for 30 min before incubation with $CoCl_2$ (100 μM) for 24 h. A, Cell lysates were electrophoresed and probed by Western blotting with antibodies specific for osteopontin (OPN) and α-tubulin. B, Serum-free culture media were collected for quantitative assessment of osteopontin (OPN) secretion. C, Cells were pretreated for 30 min with 20 and 30 μM of pyrrolidine dithiocarbamate (PDTC) before being incubated with $CoCl_2$ (100 μM) for 24 h. Serum-free culture media were collected for quantitative assessment of osteopontin (OPN) secretion. D, Cells were incubated with DCFH-DA (1 μM) for 30 min in the presence of $CoCl_2$ (100 μM), and the fluorescence intensities of metabolites were analyzed using flow cytometry as described in Materials and methods. The lower panel shows the relative fluorescence intensities, given as the means ± S.D. of 3 independent experiments. E, Cells were pretreated for 30 min with LY 294002 (10 and 20 μM), SP600125 (10 μM), or SB203580 (10 μM) before being incubated with $CoCl_2$ (100 μM) for 24 h. Serum-free culture media were collected for quantitative assessment of osteopontin secretion. F, Cells were treated with $CoCl_2$ (100 μM) for various time periods and lysed. Cell lysates were electrophoresed and probed by antibodies specific for p38MAPK, phospho-p38MAPK, Akt, or phospho-Akt (Ser^{473}). G, Cells were pretreated with *l*-N-acetylcysteine (10 mM, *l*-NAC) before being incubated with $CoCl_2$ (100 μM) for 15 min. Cell lysates were electrophoresed and probed by antibodies specific for phosphorylated p38MAPK, total p38MAPK, phospho-Akt (Ser^{473}), or α-tubulin. Data shown in panels B, C, and E are the means ± S.D. for 3 independent experiments done in triplicate. Data shown in panels A, F, and G are representative immunoblots that have been repeated twice with similar results. *Statistical differences ($P<0.05$) compared to control. #Statistical differences ($P<0.05$) compared to $CoCl_2$ (100 μM).

with rosiglitazone, dexamethasone, tanshinone IIA, celecoxib, and dipyridamole prior to treatment with $CoCl_2$. While pretreatment of cells with rosiglitazone or dexamethasone did not inhibit $CoCl_2$-induced osteopontin production (Fig. 3A, B), pretreatment with tanshinone IIA (Fig. 3C), celecoxib (Fig. 3D), or dipyridamole (Fig. 4A, B) markedly inhibited $CoCl_2$-induced osteopontin production in NRK52E cells. Tanshinone IIA (30 μM), celecoxib (10 μM) or dipyridamole (10 μM) did not affect basal osteopontin production

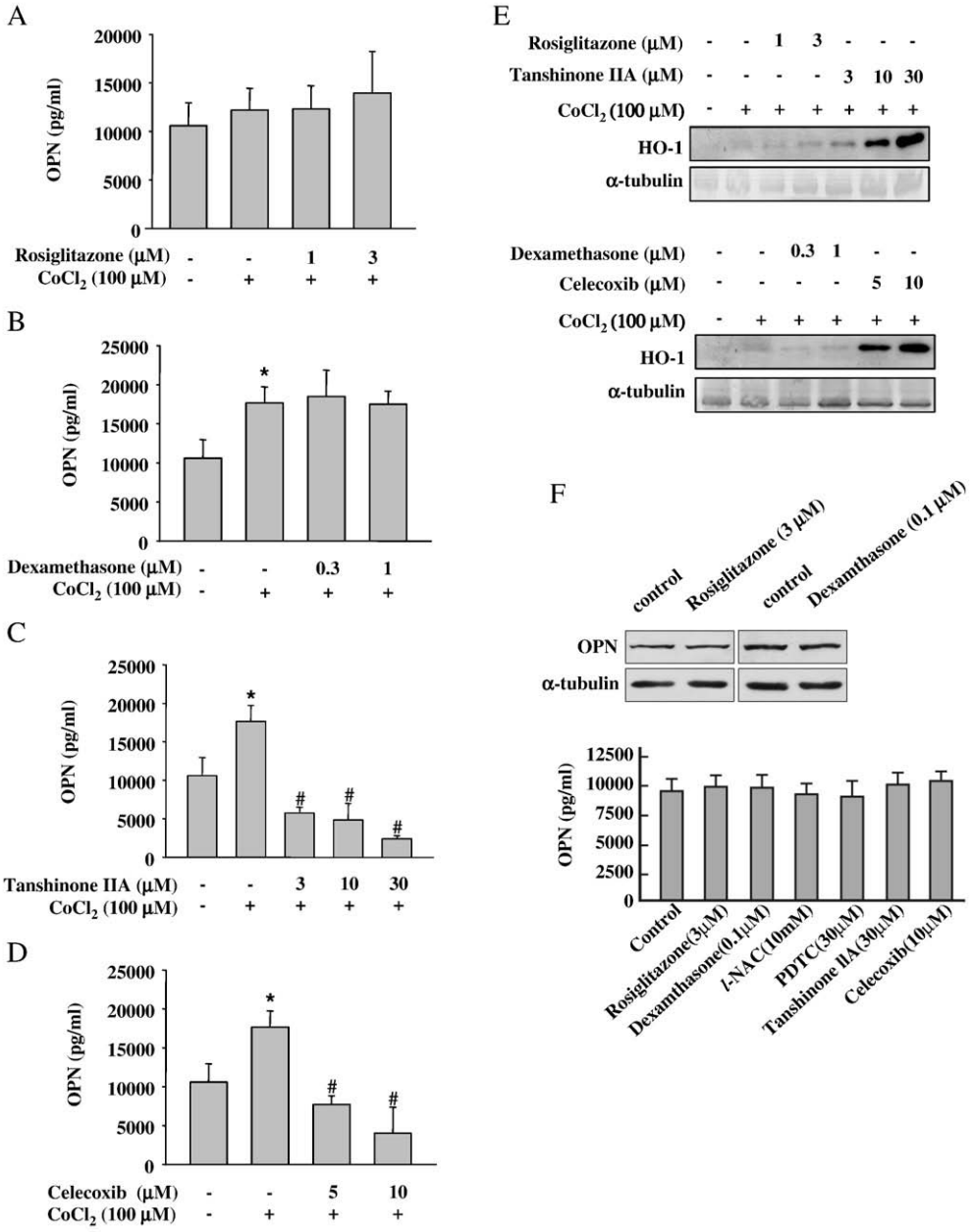

Fig. 3. Effects of anti-inflammatory agents on osteopontin production and on HO-1 expression in renal NRK52E cells. After serum starvation for 24 h, cells were incubated with A, rosiglitazone (1 and 3 μM); B, dexamethasone (0.3–1 μM); C, tanshinone IIA (3–30 μM) or D, celecoxib (5–10 μM) for 30 min before incubated with $CoCl_2$ (100 μM) for 24 h. Serum-free culture supernatants were collected for quantitative assessments of secreted osteopontin (OPN). Data shown in panels A–D are means ± S.D. for 3 independent experiments done in triplicate. E, Effects of these anti-inflammatory agents on HO-1 protein expression in NRK52E cell lysates were detected by Western blots with antibodies specific for HO-1 and α-tubulin. These experiments were all repeated with similar results. F, Effects of rosiglitazone and dexamethasone on osteopontin protein expression in NRK52E cells, and effects of anti-inflammatory agents and antioxidants on osteopontin secretion into media were examined. *Statistical differences ($P<0.05$) compared to control. #Statistical differences ($P<0.05$) compared to $CoCl_2$ (100 μM).

(Fig. 3F) or decrease the cell viability (data not shown). Because tanshinone IIA, celecoxib, and dipyridamole all induced HO-1 expression (Figs. 3E, 4E), subsequent experiments were designed to delineate the role of HO-1 in the inhibition of $CoCl_2$-induced osteopontin expression.

3.4. Dipyridamole induced HO-1 expression in NRK52E cells

Dipyridamole elicited a dose-dependent inhibition of osteopontin secretion and osteopontin protein expression in NRK52E cells (Fig. 4A, B). Notably, the inhibition of osteopontin production was associated with increased HO-1 protein expression. HO-1 induction was noticeable at 1 μM and reached a maximum at 10 μM (Fig. 4B). Dipyridamole increased HO-1 mRNA levels as demonstrated by RT-PCR (Fig. 4C) and treatment of NRK52E cells with actinomycin D (which inhibits transcription) but not cycloheximide (which inhibits translation) inhibited dipyridamole-induced HO-1 mRNA expression (Fig. 4D). Similarly, dipyridamole alone is enough to increase cellular HO-1 protein level (Fig. 4E).

3.5. Induction of HO-1 by dipyridamole is linked to inhibition of $CoCl_2$-induced osteopontin expression in NRK52E cells

To explore the mechanism further, NRK52E cells were treated with dipyridamole (10 μM) in the presence or absence of the HO-1 inhibitor, tin protoporphyrin, prior to the addition of $CoCl_2$. The

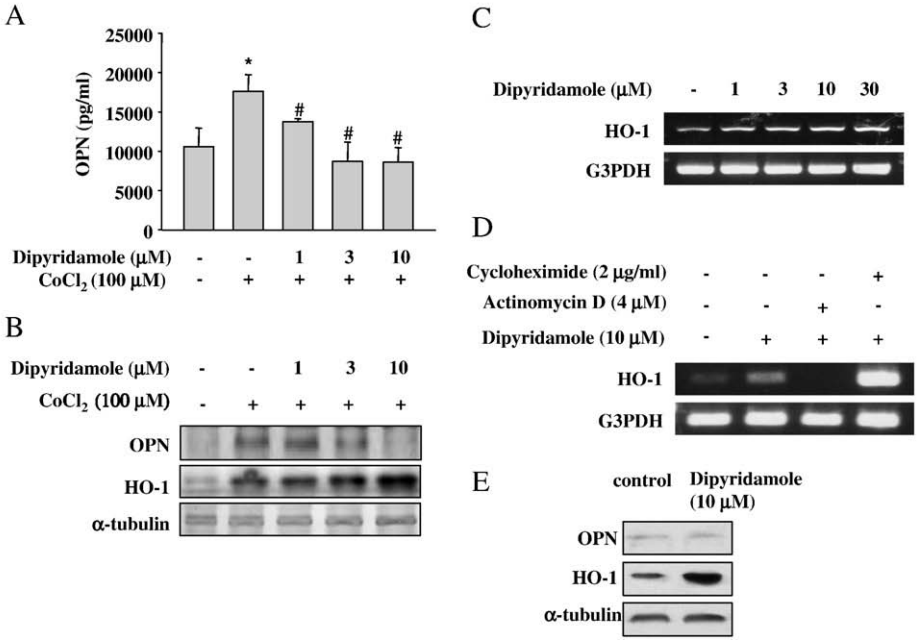

Fig. 4. Dipyridamole inhibited $CoCl_2$-induced osteopontin expression in rat NRK52E cells. After serum-starvation for 24 h, cells were pretreated with different concentrations of dipyridamole (1–10 μM) for 15 min prior to the addition of $CoCl_2$ (100 μM) for 24 h. A, Serum-free cultured media were collected for quantitative assessment of secreted osteopontin (OPN). B, Cell were lysed after incubation, and the protein expression levels of osteopontin and HO-1 were detected by Western blots with antibodies specific for osteopontin (OPN), HO-1, and α-tubulin. C, Cells were incubated with different concentrations of dipyridamole (1–10 μM), and HO-1 and G3PDH mRNA expressions were analyzed by RT-PCR as described in Materials and methods. In D, cells were pretreated with actinomycin D (4 mM) or cycloheximide (10 mM) before being incubated with dipyridamole (10 μM) for 24 h. HO-1 and G3PDH mRNA expressions were analyzed by RT-PCR. E, Effects of dipyridamole (10 μM) on osteopontin and HO-1 protein expression were detected using Western blotting assay. *Statistical differences ($P<0.05$) compared to control. #Statistical differences ($P<0.05$) compared to $CoCl_2$ (100 μM).

inhibition of osteopontin production by dipyridamole was reversed by tin protoporphyrin (Fig. 5A, B). HO-1 catalyzes the rate-limiting step in heme degradation, resulting in the formation of iron, carbon monoxide, and biliverdin. Among these reaction products, CO is known to mediate a variety of effects. To assess the role of CO in the inhibition of $CoCl_2$-induced osteopontin expression, we examined whether treatment with the tricarbonyl dichlororuthenium (II) dimer, a CO-releasing compound, could suppress $CoCl_2$-induced osteopontin expression. The CO donor mimicked dipyridamole in inhibiting $CoCl_2$-induced osteopontin expression (Fig. 5C) and secretion (Fig. 5D). To further assess the role of CO in the inhibition of $CoCl_2$-induced osteopontin expression by dipyridamole, we examined whether treatment of cells with the CO scavenger, hemoglobin, could reverse the inhibition by dipyridamole. Hemoglobin reversed the inhibition by dipyridamole (Fig. 5E, F). Collectively, these data suggest that dipyridamole may inhibit $CoCl_2$-induced osteopontin expression through a mechanism that involves the action of CO.

We previously found that dipyridamole exerts its anti-inflammatory effects via increasing MKP-1 phosphorylation (Chen et al., 2006). To test whether HO-1 induction is linked to MKP-1 phospohrylation, cells were transfected with HO-1 small interfering RNA (siRNA) and incubated in the presence or absence of dipyridamole. As shown in Fig. 6, transfection of HO-1 siRNA decreased the HO-1 protein levels in NRK52E cells. Addition of dipyridamole increased HO-1 protein expression in mock transfected cells, and this response was attenuated by transfection of HO-1 specific siRNA. Treatment of cells with $CoCl_2$ did not alter MKP-1 protein level either in the presence or absence of dipyridamole, but addition of dipyridamole increased MKP-1 phosphorylation, and this effect was blocked in HO-1 knock-down cells but not in mock transfected cells (Fig. 6). These results are consistent with the notion that MKP-1 phosphorylation is regulated by HO-1 induction.

Because p38MAPK activation mediate $CoCl_2$-induced osteopontin production, possibly dipyridamole inhibited osteopontin production by suppressing p38MAPK through MKP-1. To explore this possibility, cells were transfected with MKP-1 siRNA, and p38MAPK phosphorylation and osteopontin expression were examined in the presence or absence of dipyridamole. As shown in Fig. 7, transfection of MKP-1 siRNA markedly reduced MKP-1 protein levels in NRK52E cells. Incubation of cells with $CoCl_2$ increased p38MAPK phosphorylation and osteopontin expression, and both effects were inhibited by dipyridamole in mock transfected cells but not in MKP-1 knock-down cells. Noticeably, the level of p38MAPK phosphorylation paralleled with osteopontin expression in NRK52 E cells.

4. Discussion

In this study, we used an immortalized rat proximal tubular epithelial cell line to delineate the regulation of $CoCl_2$-induced osteopontin expression, and the possible signaling mechanisms. $CoCl_2$ is a hypoxia mimetic. We showed that $CoCl_2$-induced osteopontin expression may be mediated through PI3K/Akt and p38MAPK pathways. We found that a number of anti-inflammatory agents can be used to suppress hypoxia-induced osteopontin expression. Further, we demonstrated that many of these agents increase HO-1 expression and that dipyridamole suppressed $CoCl_2$-induced osteopontin expression via a HO-1-dependent pathway. We present evidence that the inhibition of HO-1 by tin protoporphyrin reversed dipyridamole's inhibitory effect. We show that the inhibition of $CoCl_2$-induced osteopontin upregulation by dipyridamole may be mediated through CO production, because treatment of cells with the CO-releasing molecule tricarbonyldichloro-ruthenium (II) dimer suppressed $CoCl_2$-induced osteopontin expression, and because removal of CO by hemoglobin, a CO scavenger, partly reversed dipyridamole's inhibitory effect on osteopontin induction. Furthermore, we demonstrated that knockdown of either HO-1 or MKP-1 reversed dipyridamole's inhibitory effect on osteopontin induction. Thus, dipyridamole may inhibit 38MAPK phosphorylation and osteopontin production via a HO-1/CO/MKP-1-dependent mechanism.

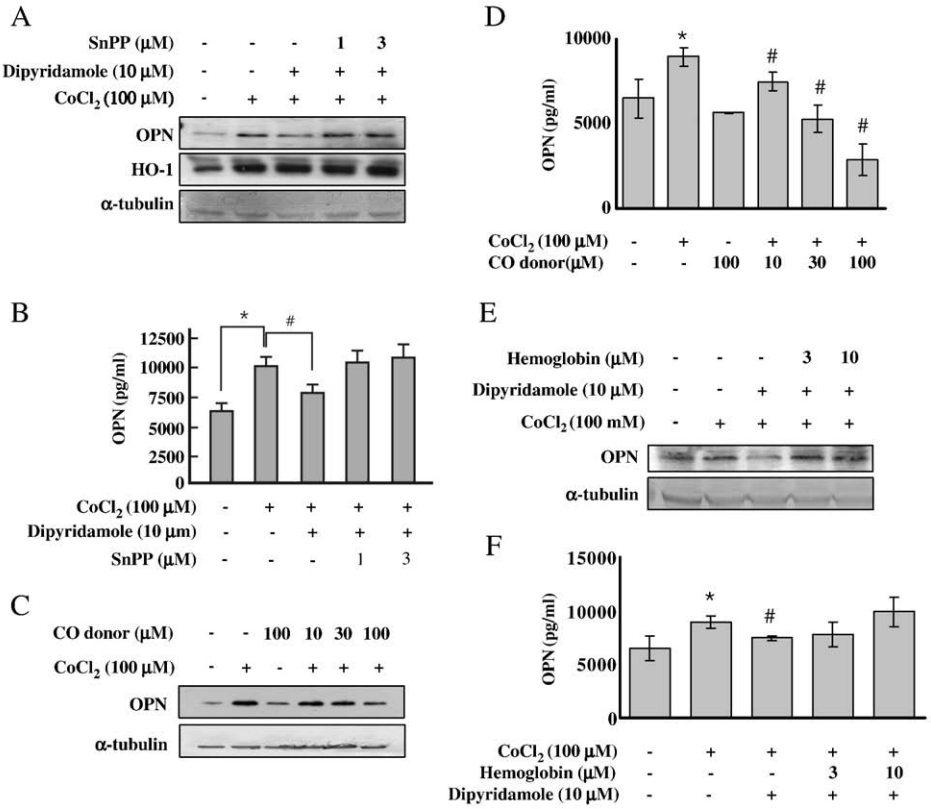

Fig. 5. Heme oxygenase-1 is involved in the reduction of $CoCl_2$-induced osteopontin expression in NRK52E cells. A, After serum starvation for 24 h, cells were pretreated with indicated concentrations of tin protoporphyrin (SnPP) for 15 min before incubation without or with $CoCl_2$ (100 μM) in the absence or presence of dipyridamole for 24 h. Cells were lysed and the protein levels of osteopontin and HO-1 were detected by Western blots with antibodies specific for osteopontin (OPN), HO-1, and α-tubulin. B, The effects of the inhibitor for HO-1, tin protoporphyrin, on osteopontin secretion were detected using ELISA in NRK-52E cells treated with $CoCl_2$ and dipyridamole. C, NRK52E cells were pretreated with different concentrations of the tricarbonyl dichlororuthenium (II) dimer (10, 30, and 100 μM, CO donor) for 30 min before the addition of $CoCl_2$ (100 μM) for 24 h. D, Serum-free cultured media were collected for quantitative assessment of secreted osteopontin (OPN). E, Cells were pretreated with the indicated concentrations of hemoglobin for 15 min before being incubated without or with dipyridamole (10 μM), in the absence or presence of $CoCl_2$ (100 μM) for 24 h; F, Serum-free cultured media were collected for quantitative assessment of secreted osteopontin (OPN). Data shown in panels B, D and F are the means ± S.D. for 3 independent experiments done in triplicate. Data shown in panels A, C, and E are representative immunoblots that have been repeated twice with similar results. *Statistical differences ($P<0.05$) compared to control. #Statistical differences ($P<0.05$) compared to $CoCl_2$ (100 μM).

Osteopontin protein and gene expressions were elevated after ischemia and reperfusion in an *ex vivo* hemoperfusion model (Kossmehl et al., 2005). We demonstrated that incubation of rat kidney tubular epithelial cells with $CoCl_2$ resulted in marked elevation of osteopontin protein and gene expressions. $CoCl_2$ has been shown to mimic hypoxic responses in various cell lines and to cause the overproduction of reactive oxygen species (Gaitanaki et al., 2007; Lu et al., 2007). In agreement, we showed that incubation of NRK52E cells with $CoCl_2$ increased reactive oxygen species production. Mitogen-activated protein kinases (MAPKs) constitute one of the most important intracellular signaling pathways. In particular, the p38MAPK subfamily is known to be activated under various stressful conditions, such as mechanical or oxidative stress. We showed that

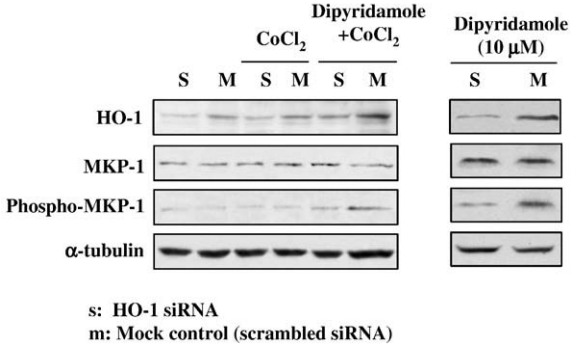

Fig. 6. Dipyridamole increased MKP-1 phosphorylation via HO-1 induction. NRK52E cells were transfected with either HO-1 small interfering RNA (siRNA) (20 nM) or scrambled siRNA as a mock control and treated without or with dipyridamole (10 μM) for 30 min prior to incubation with $CoCl_2$ for 24 h. Cell lysates were immunoblotted with antibodies specific for HO-1, total MKP-1, phosphorylated MKP-1, or α-tubulin. This experiment was repeated with similar results.

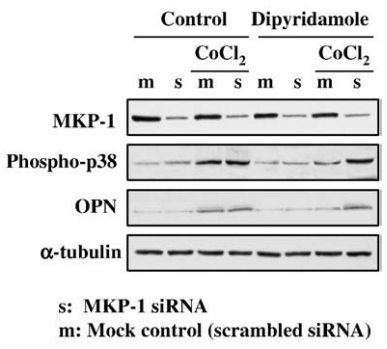

Fig. 7. Dipyridamole regulates $CoCl_2$-induced osteopontin expression via MKP-1. NRK52E cells were either transfected with MKP-1 small interfering RNA (siRNA) (20 nM) or with scrambled siRNA as a mock control and incubated without or with dipyridamole (10 μM) for 24 h. Cell lysates were immunoblotted with antibodies specific for MKP-1, phosphorylated p38MAPK, osteopontin (OPN), or α-tubulin. This experiment was repeated with similar results.

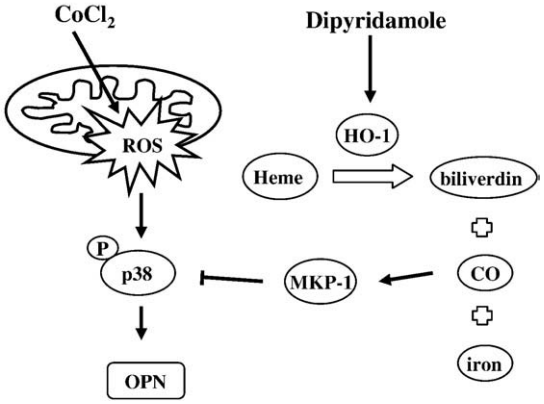

Fig. 8. Schematic diagram illustrating the signaling pathways involved in $CoCl_2$-induced osteopontin expression, and the proposed mechanism by which dipyridamole inhibits $CoCl_2$-induced osteopontin expression in NRK52E cells. Dipyridamole may inhibit $CoCl_2$-induced osteopontin expression through induction of HO-1. Induction of HO-1 in turn leads to generation of CO, bilirubin, and Fe^{2+}. CO may suppress osteopontin expression via MKP-1 activation.

treatment of NRK52E cells with $CoCl_2$ increased p38MAPK phosphorylation, and this effect was attenuated by *l*-N-acetylcysteine. Our data are consistent with two recent reports showing that $CoCl_2$ activates the p38MAPK signaling pathway (Gaitanaki et al., 2007; Lu et al., 2007). Incubation of cells with SB203580 or *l*-N-acetylcysteine inhibited $CoCl_2$-induced osteopontin expression suggesting the osteopontin induction is mediated through a reactive oxygen species- and p38MAPK-dependent pathway. On the other hand, $CoCl_2$-induced osteopontin expression was inhibited by Ly204002, an inhibitor specific for PI3 kinase. Although similar kinase activation was observed for Akt phosphorylation, Akt phosphorylation was not inhibited by pretreating NRK52E cells with the antioxidant, *l*-N-acetylcysteine. Recently, it has been shown that both endogenous and exogenous osteopontin expression activates PI3 kinase/Akt signaling pathway (Song et al., 2008). One possible explanation is that PI3 kinase/Akt activation is secondary to osteopontin secretion. Nevertheless reactive oxygen species are required for osteopontin expression, because pretreatment of *l*-N-acetylcysteine or PDTC (which is also an antioxidant) suppresses osteopontin secretion to less than control levels (Fig. 2B, C). These results suggest that $CoCl_2$-induced osteopontin expression may be mediated through a reactive oxygen species- and p38MAPK-dependent pathway or a reactive oxygen species-independent PI3 kinase/Akt pathway.

Osteopontin was shown to play a deleterious role in the progression of renal fibrosis (Kramer et al., 2005; Yoo et al., 2006), liver fibrosis (Lorena et al., 2006) and pulmonary fibrosis (Pardo et al., 2005). Knockout of osteopontin prevents cardiac hypertrophy and fibrosis *in vitro* and *in vivo* (Graf and Stawowy, 2004). It is conceivable that therapeutic agents that suppress hypoxia-induced osteopontin production may be useful for attenuating the fibrotic process associated with renal ischemia. For example, in chronic cyclosporine-induced nephropathy, upregulation of tubular osteopontin expression is closely associated with macrophage influx and renal scarring (Pichler et al., 1995; Young et al., 1995). Administration of pravastatin effectively abrogates the progression of tubulointerstitial inflammation and fibrosis, and this renoprotective effect may be mediated by downregulating the expression of osteopontin in chronic cyclosporine-induced nephropathy (Li et al., 2005). In the present study, we showed that a number of anti-inflammatory agents, including dexamethasone, tanshinone IIA, celecoxib, and dipyridamole, can be used to suppress osteopontin expression. Our data agree with those published by Hung et al. (2001a,b,c) showing that dipyridamole inhibits the fibrogenic effect of peritoneal mesothelial cells and the accompanying accumulation of extracellular matrix in the peritoneal fibrosing syndrome.

HO-1 is a critical enzyme that evokes adaptive and cytoprotective responses in the presence of a variety of cellular stresses, including oxidative stress (Choi and Alam, 1996). Induction of HO-1 decreases the profibrotic effects in renal fiborsis (Gaedeke et al., 2005; Mark et al., 2005) and pulmonary fibrosis (Zhou et al., 2005). In agreement, treatment of cells with various anti-inflammatory agents dramatically enhanced HO-1 protein expression. Increased HO-1 expression is linked to the inhibition of $CoCl_2$-induced osteopontin expression, because treatment of cells with the HO-1 competitive inhibitor, tin protoporphyrin, reversed the inhibitory effect on osteopontin mRNA transcription and secretion. Further, tricarbonyl dichlororuthenium (II) dimer, a CO-releasing compound, mimicked dipyridamole in inhibiting $CoCl_2$-induced osteopontin expression, and that the scavenging of CO by hemoglobin reversed the inhibition by dipyridamole. Collectively, these data suggest that dipyridamole can regulate osteopontin secretion through a mechanism that involves the action of CO. Although the detail mechanisms remained to be explored, our data suggest activation of MKP-1 may contribute to the inhibition of $CoCl_2$-induced osteopontin expression by dipyridamole.

In conclusion, we demonstrated that $CoCl_2$ treatment increases reactive oxygen species generation, which in turn activates p38MAPK and induces osteopontin expression. Dipyridamole may inhibit $CoCl_2$-induced osteopontin expression through HO-1 induction. Induction of HO-1 expression is associated with increased CO production and MKP-1 phosphorylation. Possibly phosphorylation and activation of MKP-1 dephosphorates p38MAPK and thus suppresses osteopontin expression. Fig. 8 shows a schematic illustration of these findings.

References

Alvarez-Maqueda, M., El Bekay, R., Alba, G., Monteseirin, J., Chacon, P., Vega, A., Martin-Nieto, J., Bedoya, F.J., Pintado, E., Sobrino, F., 2004. 15-deoxy-delta 12,14-prostaglandin J2 induces heme oxygenase-1 gene expression in a reactive oxygen species-dependent manner in human lymphocytes. J. Biol. Chem. 279, 21929–21937.

Ashkar, S., Weber, G.F., Panoutsakopoulou, V., Sanchirico, M.E., Jansson, M., Zawaideh, S., Rittling, S.R., Denhardt, D.T., Glimcher, M.J., Cantor, H., 2000. Eta-1 (osteopontin): an early component of type-1 (cell-mediated) immunity. Science 287, 860–864.

Basile, D.P., Fredrich, K., Alausa, M., Vio, C.P., Liang, M., Rieder, M.R., Greene, A.S., Cowley Jr., A.W., 2005. Identification of persistently altered gene expression in the kidney after functional recovery from ischemic acute renal failure. Am. J. Physiol., Renal Physiol. 288, F953–F963.

Bender, A.T., Beavo, J.A., 2006. Cyclic nucleotide phosphodiesterases: molecular regulation to clinical use. Pharmacol. Rev. 58, 488–520.

Chandel, N.S., McClintock, D.S., Feliciano, C.E., Wood, T.M., Melendez, J.A., Rodriguez, A.M., Schumacker, P.T., 2000. Reactive oxygen species generated at mitochondrial complex III stabilize hypoxia-inducible factor-1alpha during hypoxia: a mechanism of O2 sensing. J. Biol. Chem. 275, 25130–25138.

Chen, T.H., Kao, Y.C., Chen, B.C., Chen, C.H., Chan, P., Lee, H.M., 2006. Dipyridamole activation of mitogen-activated protein kinase phosphatase-1 mediates inhibition of lipopolysaccharide-induced cyclooxygenase-2 expression in RAW 264.7 cells. Eur. J. Pharmacol. 541, 138–146.

Choi, A.M., Alam, J., 1996. Heme oxygenase-1: function, regulation, and implication of a novel stress-inducible protein in oxidant-induced lung injury. Am. J. Respir. Cell Mol. Biol. 15, 9–19.

Choi, J.S., Kim, H.Y., Cha, J.H., Choi, J.Y., Lee, M.Y., 2007. Transient microglial and prolonged astroglial upregulation of osteopontin following transient forebrain ischemia in rats. Brain Res. 1151, 195–202.

Dubey, R.K., Gillespie, D.G., Jackson, E.K., 1999. Adenosine inhibits collagen and total protein synthesis in vascular smooth muscle cells. Hypertension 33, 190–194.

Gaedeke, J., Noble, N.A., Border, W.A., 2005. Curcumin blocks fibrosis in anti-Thy 1 glomerulonephritis through up-regulation of heme oxygenase 1. Kidney Int. 68, 2042–2049.

Gaitanaki, C., Kalpachidou, T., Aggeli, I.K., Papazafiri, P., Beis, I., 2007. $CoCl_2$ induces protective events via the p38-MAPK signalling pathway and ANP in the perfused amphibian heart. J. Exp. Biol. 210, 2267–2277.

Giachelli, C.M., Pichler, R., Lombardi, D., Denhardt, D.T., Alpers, C.E., Schwartz, S.M., Johnson, R.J., 1994. Osteopontin expression in angiotensin II-induced tubulointerstitial nephritis. Kidney Int. 45, 515–524.

Graf, K., Stawowy, P., 2004. Osteopontin: a protective mediator of cardiac fibrosis? Hypertension 44, 809–810.

Hammond, J.R., Stolk, M., Archer, R.G., McConnell, K., 2004. Pharmacological analysis and molecular cloning of the canine equilibrative nucleoside transporter 1. Eur. J. Pharmacol. 491, 9–19.

Hung, K.Y., Chen, C.T., Huang, J.W., Lee, P.H., Tsai, T.J., Hsieh, B.S., 2001a. Dipyridamole inhibits TGF-beta-induced collagen gene expression in human peritoneal mesothelial cells. Kidney Int. 60, 1249–1257.

Hung, K.Y., Chen, C.T., Yen, C.J., Lee, P.H., Tsai, T.J., Hsieh, B.S., 2001b. Dipyridamole inhibits PDGF-stimulated human peritoneal mesothelial cell proliferation. Kidney Int. 60, 872–881.

Hung, K.Y., Shyu, R.S., Fang, C.C., Tsai, C.C., Lee, P.H., Tsai, T.J., Hsieh, B.S., 2001c. Dipyridamole inhibits human peritoneal mesothelial cell proliferation in vitro and attenuates rat peritoneal fibrosis in vivo. Kidney Int. 59, 2316–2324.

Iguchi, S., Nishi, S., Ikegame, M., Hoshi, K., Yoshizawa, T., Kawashima, H., Arakawa, M., Ozawa, H., Gejyo, F., 2004. Expression of osteopontin in cisplatin-induced tubular injury. Nephron Exp. Nephrol. 97, e96–e105.

Khanna, A., Plummer, M., Bromberek, C., Bresnahan, B., Hariharan, S., 2002. Expression of TGF-beta and fibrogenic genes in transplant recipients with tacrolimus and cyclosporine nephrotoxicity. Kidney Int. 62, 2257–2263.

Kossmehl, P., Schonberger, J., Shakibaei, M., Faramarzi, S., Kurth, E., Habighorst, B., von Bauer, R., Wehland, M., Kreutz, R., Infanger, M., Schulze-Tanzil, G., Paul, M., Grimm, D., 2005. Increase of fibronectin and osteopontin in porcine hearts following ischemia and reperfusion. J. Mol. Med. 83, 626–637.

Kramer, A.B., Ricardo, S.D., Kelly, D.J., Waanders, F., van Goor, H., Navis, G., 2005. Modulation of osteopontin in proteinuria-induced renal interstitial fibrosis. J. Pathol. 207, 483–492.

Lan, H.Y., Yu, X.Q., Yang, N., Nikolic-Paterson, D.J., Mu, W., Pichler, R., Johnson, R.J., Atkins, R.C., 1998. De novo glomerular osteopontin expression in rat crescentic glomerulonephritis. Kidney Int. 53, 136–145.

Levin, A., 1999. Management of membranoproliferative glomerulonephritis: evidence-based recommendations. Kidney Inter., Suppl. 70, S41–S46.

Li, C., Sun, B.K., Lim, S.W., Song, J.C., Kang, S.W., Kim, Y.S., Kang, D.H., Cha, J.H., Kim, J., Yang, C.W., 2005. Combined effects of losartan and pravastatin on interstitial inflammation and fibrosis in chronic cyclosporine-induced nephropathy. Transplantation 79, 1522–1529.

Lien, Y.H., Lai, L.W., Silva, A.L., 2003. Pathogenesis of renal ischemia/reperfusion injury: lessons from knockout mice. Life Sci. 74, 543–552.

Lorena, D., Darby, I.A., Gadeau, A.P., Leen, L.L., Rittling, S., Porto, L.C., Rosenbaum, J., Desmouliere, A., 2006. Osteopontin expression in normal and fibrotic liver. Altered liver healing in osteopontin-deficient mice. J. Hepatol. 44, 383–390.

Lu, N., Zhou, H., Lin, Y.H., Chen, Z.Q., Pan, Y., Li, X.J., 2007. Oxidative stress mediates CoCl (2)-induced prostate tumour cell adhesion: role of protein kinase C and p38 mitogen-activated protein kinase. Basic Clin. Pharmacol. Toxicol. 101, 41–46.

Malyankar, U.M., Almeida, M., Johnson, R.J., Pichler, R.H., Giachelli, C.M., 1997. Osteopontin regulation in cultured rat renal epithelial cells. Kidney Int. 51, 1766–1773.

Mark, A., Hock, T., Kapturczak, M.H., Agarwal, A., Hill-Kapturczak, N., 2005. Induction of heme oxygenase-1 modulates the profibrotic effects of transforming growth factor-beta in human renal tubular epithelial cells. Cell. Mol. Biol. (Noisy-le-grand) 51, 357–362.

Nolin, L., Courteau, M., 1999. Management of IgA nephropathy: evidence-based recommendations. Kidney Inter., Suppl. 70, S56–S62.

Norman, J.T., Clark, I.M., Garcia, P.L., 2000. Hypoxia promotes fibrogenesis in human renal fibroblasts. Kidney Int. 58, 2351–2366.

Otterbein, L.E., Choi, A.M., 2000. Heme oxygenase: colors of defense against cellular stress. Am. J. Physiol., Lung Cell. Mol. Physiol. 279, L1029–L1037.

Pardo, A., Gibson, K., Cisneros, J., Richards, T.J., Yang, Y., Becerril, C., Yousem, S., Herrera, I., Ruiz, V., Selman, M., Kaminski, N., 2005. Up-regulation and profibrotic role of osteopontin in human idiopathic pulmonary fibrosis. PLoS Med. 2, e251.

Persy, V.P., Verhulst, A., Ysebaert, D.K., De Greef, K.E., De Broe, M.E., 2003. Reduced postischemic macrophage infiltration and interstitial fibrosis in osteopontin knockout mice. Kidney Int. 63, 543–553.

Pichler, R.H., Franceschini, N., Young, B.A., Hugo, C., Andoh, T.F., Burdmann, E.A., Shankland, S.J., Alpers, C.E., Bennett, W.M., Couser, W.G., 1995. Pathogenesis of cyclosporine nephropathy: roles of angiotensin II and osteopontin. J. Am. Soc. Nephrol. 6, 1186–1196.

Song, G., Cai, Q.F., Mao, Y.B., Ming, Y.L., Bao, S.D., Ouyang, G.L., 2008. Osteopontin promotes ovarian cancer progression and cell survival and increases HIF-1alpha expression through the PI3-K/Akt pathway. Cancer Sci. 99, 1901–1907.

Stafford, N.P., Pink, A.E., White, A.E., Glenn, J.R., Heptinstall, S., 2003. Mechanisms involved in adenosine triphosphate-induced platelet aggregation in whole blood. Arterioscler. Thromb. Vasc. Biol. 23, 1928–1933.

Thomas, S.E., Lombardi, D., Giachelli, C., Bohle, A., Johnson, R.J., 1998. Osteopontin expression, tubulointerstitial disease, and essential hypertension. Am. J. Hypertens. 11, 954–961.

Xie, Y., Sakatsume, M., Nishi, S., Narita, I., Arakawa, M., Gejyo, F., 2001. Expression, roles, receptors, and regulation of osteopontin in the kidney. Kidney Int. 60, 1645–1657.

Yoo, K.H., Thornhill, B.A., Forbes, M.S., Coleman, C.M., Marcinko, E.S., Liaw, L., Chevalier, R.L., 2006. Osteopontin regulates renal apoptosis and interstitial fibrosis in neonatal chronic unilateral ureteral obstruction. Kidney Int. 70, 1735–1741.

Young, B.A., Burdmann, E.A., Johnson, R.J., Alpers, C.E., Giachelli, C.M., Eng, E., Andoh, T., Bennett, W.M., Couser, W.G., 1995. Cellular proliferation and macrophage influx precede interstitial fibrosis in cyclosporine nephrotoxicity. Kidney Int. 48, 439–448.

Zhou, Z., Song, R., Fattman, C.L., Greenhill, S., Alber, S., Oury, T.D., Choi, A.M., Morse, D., 2005. Carbon monoxide suppresses bleomycin-induced lung fibrosis. Am. J. Pathol. 166, 27–37.